Nonlinear Processes in Geophysics (2003) 10: 425–434

Nonlinear Processes in Geophysics

The choice of optimal Discrete Interaction Approximation to the kinetic integral for ocean waves

V. G. Polnikov

Obukhov Institute for Atmospheric Physics of Russian Academy of Sciences, Pyzhevskki lane 3, Moscow, 109017, Russia

Received: 18 September 2002 – Revised: 3 February 2003 – Accepted: 7 February 2003

Abstract. A lot of discrete configurations for the four-wave nonlinear interaction processes have been calculated and tested by the method proposed earlier in the frame of the concept of Fast Discrete Interaction Approximation to the Hasselmann's kinetic integral (Polnikov and Farina, 2002). It was found that there are several simple configurations, which are more efficient than the one proposed originally in Hasselmann et al. (1985). Finally, the optimal multiple Discrete Interaction Approximation (DIA) to the kinetic integral for deep-water waves was found. Wave spectrum features have been intercompared for a number of different configurations of DIA, applied to a long-time solution of kinetic equation. On the basis of this intercomparison the better efficiency of the configurations proposed was confirmed. Certain recommendations were given for implementation of new approximations to the wave forecast practice.

1 Introduction

It is well known that the nonlinear wave-wave interactions play a principally important role in the wind waves evolution (Young and van Vledder, 1993; Komen et al., 1994). Under some constraints they are described by the so-called four-wave kinetic integral of the form

$$\begin{aligned}\frac{\partial N(\boldsymbol{k}_4)}{\partial t} &\equiv T_N(\boldsymbol{k}) \\ &= 4\pi \int d\boldsymbol{k}_1 \int d\boldsymbol{k}_2 \int d\boldsymbol{k}_3 M^2(\boldsymbol{k}_1, \boldsymbol{k}_2, \boldsymbol{k}_3, \boldsymbol{k}_4) \\ &\times \Big[N(\boldsymbol{k}_1) N(\boldsymbol{k}_2) \Big(N(\boldsymbol{k}_3) + N(\boldsymbol{k}_4) \Big) \\ &- N(\boldsymbol{k}_3) N(\boldsymbol{k}_4) \Big(N(\boldsymbol{k}_1) + N(\boldsymbol{k}_2) \Big) \Big] \\ &\times \delta\Big(\sigma(k_1) + \sigma(k_2) - \sigma(k_3) - \sigma(k_4) \Big) \\ &\delta(\boldsymbol{k}_1 + \boldsymbol{k}_2 - \boldsymbol{k}_3 - \boldsymbol{k}_4) \end{aligned} \quad (1)$$

derived for the first time by Hasselmann (1962). In Eq. (1) $N(\boldsymbol{k}_1)$ is the wave action spectrum, $\boldsymbol{k}_i (i = 1, 2, 3, 4)$ are the wave vectors of interacting waves, $\sigma_i \equiv \sigma(\boldsymbol{k}_i)$ are the corresponding angular frequencies of the waves due to dispersion relation, $T_N(\boldsymbol{k})$ is the nonlinear transfer of wave action, and $M(...)$ are the matrix elements describing an intensity of interaction of four waves. In this paper the relation

$$\sigma(\boldsymbol{k}) = (gk)^{1/2} \quad (2)$$

will be used, which is valid for the ocean surface gravity waves (g is the gravity acceleration).

The delta-functions in Eq. (1) assure that the four interacting waves should meet the following resonance conditions

$$\boldsymbol{k}_1 + \boldsymbol{k}_2 = \boldsymbol{k}_3 + \boldsymbol{k}_4 \,, \quad (3)$$

$$\sigma_1 + \sigma_2 = \sigma_3 + \sigma_4 \,. \quad (4)$$

A joint solution of Eqs. (2–4) defines a resonance 3-D-surface in the 8-dimensional $\boldsymbol{k}$-space. In a discrete representation, this surface gives rise to a set of 4–wave configurations for wave vectors contributing to the real nonlinear transfer of wave action (and energy as well) among waves.

Due to the very complicated form of kinetic integral in Eq. (1), in practical wind wave models this integral is substituted by some kind of approximation. At present, this point is very well elaborated, and the only problem is to find the optimal approximation to the kinetic integral, which has the best balance of accuracy and speed of calculations. This problem was considered in detail in our previous paper (Polnikov and Farina, 2002), where one can find a good list of proper references.[1]

On the basis of specially constructed mathematical measures and definitions (which is called PF-methodic), the authors of PF have shown that among different modern approximations of the kinetic integral the best one is the so-called Discrete Interaction Approximation (DIA), proposed in Hasselmann et al. (1985). We will not dwell on the DIA, as far as it is well described in the literature (for example, see Komen

Correspondence to: V. G. Polnikov
(polnikov@cptec.inpe.br; polnikov@mail.ru)

[1] Hereafter it is referred to as PF

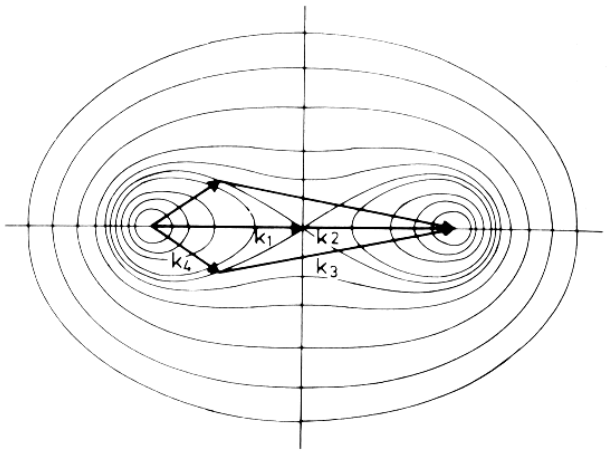

Fig. 1. Visual representation of the configuration used in DIA. Contour lines correspond to the possible end points of interacting vectors permitted by Eqs. (3) and (4).

et al., 1994; Hashimoto and Kawagushi, 2001; Van Vledder, 2001; PF). But we mention that the original DIA requests some interpolation procedures for the spectrum function under the integral in Eq. (1), provided by a mismatch of the integration grid nodes and location of some interacting wave vectors used in the DIA configuration. In PF the concept of a fast DIA (FDIA) was proposed, which does not need the interpolation procedure. The FDIA concept permits one to increase several times (at least two times) the speed of the calculation in the DIA, preserving the same accuracy if the integration grid is rather fine.

In this paper the FDIA concept is used in the frame of PF-methodic with the aim to find the optimal approximation to the kinetic integral. The outline of the paper is the following. In Sect. 2 the FDIA concept is described briefly. The principal formulas of the PF-methodic are presented in Sect. 3. The set of configurations investigated is described and classified in Sect. 4. Results of configuration testing by the PF-methodic are given in Sect. 5. In Sect. 6 the long-term spectrum evolution features are intercompared for different approximations of the kinetic equation Eq. (1). Section 7 is devoted to conclusions and recommendations.

2 The concept of the fast Discrete Interaction Approximation

As it was shown in PF, all modern, theoretically grounded and effective approximations are based on using in the six-fold integral (1) only the interacting wave-wave configurations located at the singular sub-surface of the 3-D-resonance surface defined by resonance conditions (3) and (4). An example of such a configuration used in the original DIA (Hasselmann et al., 1985) is shown in Fig. 1.

The main idea of FDIA is to use such types configurations, which are adjusted to the integration grid for the integral in Eq. (1). Thus, first of all, one should introduce the principal parameters of the grid. Then, the features of configurations in FDIA could be described.

An integration grid for the kinetic integral will be considered in the polar coordinates, where each of the interacting wave vector $\boldsymbol{k}_i (i = 1, 2, 3, 4)$ is represented by the frequency-angular point (σ_i, θ_i). In our case, the integration grid is given by the formulas

$$\sigma(I) = \sigma_0 \cdot e^{I-1} \qquad (1 \le I \le N)\,, \tag{5a}$$

$$\theta(J) = -\pi + (J-1)\cdot\Delta\theta \qquad (1 \le J \le M \text{ and } \Delta\theta = 2\pi/m). \tag{5b}$$

Thus, parameters of the grid are as follows: the lowest frequency, σ_0; the frequency exponential increment, e; the maximum number of frequencies, N; the angle resolution in radians, $\Delta\theta$; and the maximum number of angles, M. To our aims, the principal parameters are e and $\Delta\theta$, as far as they define the resolution of the grid. The numbers N and M should be rather large (several tens), but for the concept under consideration their explicit values are not principal. Note only that the FDIA concept is valid for the rather fine grid when

$$e \le 1.1 \qquad \text{and} \qquad \Delta\theta \le \pi/10\,. \tag{6}$$

Everywhere below restriction (6) should be met. Particularly, in our further consideration, the resolution parameters have values

$$e = 1.05 \qquad \text{and} \qquad \Delta\theta \le \pi/18\,, \tag{7}$$

what is related to the 'standard' integration grid introduced in PF for the exact calculation of the kinetic integral (1).

In the FDIA the basic (simple) configuration is described by the following ratios:

$$1) \qquad \boldsymbol{k}_4 = \boldsymbol{k}\,, \tag{8a}$$

where the current wave vector $\boldsymbol{k}$ is located at the grid node and represented in the polar coordinates by the proper frequency σ and angle θ;

$$2) \qquad \boldsymbol{k}_3 = \boldsymbol{k}_+\,, \tag{8b}$$

where $\boldsymbol{k}_+$ is represented by $\sigma_3 = \sigma(1+\alpha_{34})$ and $\theta_3 = \theta + \Delta\theta_{34}$;

$$3) \qquad \boldsymbol{k}_1 \approx \boldsymbol{k}_2 \approx (\boldsymbol{k}_4 + \boldsymbol{k}_3)/2 \equiv \boldsymbol{k}_a/2\,, \tag{8c}$$

where $\boldsymbol{k}_a$ is directed along the angle $\theta_a = \theta + \Delta\theta_{a4}$ and its value is given by formula (12).

Thus, we have two main parameters of configuration: the frequency increment α_{34}, defining the value of σ_3, and the proper angular increment $\Delta\theta_{34}$, defining the angle between vectors $\boldsymbol{k}_4$ and $\boldsymbol{k}_3$. By varying these parameters, one can vary the configuration as a whole (including the values of $\boldsymbol{k}_a$ and θ_a) due to Eq. (3).

The main differences between the configurations used in FDIA and in the original DIA are as follows:

(a) all wave vectors $\boldsymbol{k}_1, \boldsymbol{k}_2, \boldsymbol{k}_3$, and $\boldsymbol{k}_4$ should be allocated at the nodes of the integration grid;

(b) vectors $\boldsymbol{k}_1$ and $\boldsymbol{k}_2$ may be unequal, i.e. they may have some (but small) discrepancies both in values and in directions;

(c) the resonance conditions (3) and (4) may be met rather approximately than exactly.

The main common feature of all the configurations is that they are allocated in the vicinity of the 'figure-of-eight' in the $\boldsymbol{k}$-space (see, Fig. 1). This requirement is expressed by the following ratios (Polnikov, 1989):

$$k_a = \sigma_a^2/2 \,, \tag{9}$$

where

$$k_a = \left[\sigma^4 + \sigma_3^4 + 2\sigma^2\sigma_3^2 \cos\left(\Delta\theta_{34}\right)\right]^{1/2} , \tag{10}$$

and

$$\sigma_a = \sigma + \sigma_3 \,. \tag{11}$$

Equations (9)–(11) determine the value of increment $\Delta\theta_{34}$, for the given σ and σ_3. After that, the expression for $\Delta\theta_{a4}$ is deduced from the resonant condition (3):

$$\Delta\theta_{a4} = \mathrm{arctg}\left[\frac{\sigma_3^2 \sin\left(\Delta\theta_{34}\right)}{\sigma_3^2 \cos\left(\Delta\theta_{34}\right) + \sigma^2}\right] . \tag{12}$$

To fix the FDIA configuration, it needs to define several integer values corresponding to requirement (a) mentioned above (allocation of the vectors on the grid). This requirement can be expressed by the following equations:

$$\sigma_3 = \sigma \cdot e^{m3}, \qquad \sigma_1 = \sigma \cdot e^{m1}, \qquad \sigma_2 = \sigma \cdot e^{m2} \,, \tag{13a}$$

and

$$\Delta\theta_{34} = n3 \cdot \Delta\theta \,, \qquad \Delta\theta_{a4} = na \cdot \Delta\theta \,. \tag{13b}$$

where $n3$ and na are found from the previously estimated $\Delta\theta_{34}$ and $\Delta\theta_{a4}$ by formulas

$$n3 = \mathrm{Int}(\Delta\theta_{34}/\Delta\theta) \,, \quad na = \mathrm{Int}(\Delta\theta_{a4}/\Delta\theta) \,. \tag{13c}$$

Here, $m1, m2, n3$, and na are the integer values to be found for any given integer $m3$; and the function Int(...) represents the integer number which is nearest to the argument.

Requirement (b) mentioned above (inequality of vectors $\boldsymbol{k}_1$ and $\boldsymbol{k}_2$) means that one can use the following choice for modulus parameters of the vectors $\boldsymbol{k}_1$ and $\boldsymbol{k}_2$:

$$m1 = m2 \qquad \text{or} \qquad m1 = m2 \pm 1 \,, \tag{14}$$

and the corresponding choice for the angle parameters of the vectors $\boldsymbol{k}_1$ and $\boldsymbol{k}_2$:

$$n2,\ n3 = na \qquad \text{or} \qquad n2,\ n3 = na \pm 1 \,, \tag{15}$$

where $n2, n3$ are the angular parameters of the vectors $\boldsymbol{k}_1$ and $\boldsymbol{k}_2$ corresponding to Eqs. (8c) and (13c).

Hereby the algorithm of the FDIA configuration calculations is totally described. The set of configurations under investigation will be presented in Sect. 3.

3 PF-methodic of approximation efficiency estimation

The term 'efficiency of approximation' was specified in detail in PF. It is based on the rigorous formula for the averaged relative error of approximation (ARE), $< \epsilon_{\mathrm{rel}} >$, and phenomenological formula for the efficiency, Eff. In turn, the value ϵ_{rel} (defined below) is named as a mean relative error (MRE). There are two situations, and the formulas for them are as follows.

For a simple FDIA configuration[2]

$$Eff_1 = \left(< \epsilon_{\mathrm{rel}} > \right)^{-2} . \tag{16}$$

In the case of a multiple FDIA configuration, the efficiency is estimated by the formula

$$Eff_1 = \left(< \epsilon_{\mathrm{rel}} > \right)^{-2} \left(N_c\right)^{-RP} , \tag{17}$$

where N_c is the number of simple configurations in a multiple one, and RP is the so-called relative part of CPU time, taken by the nonlinear sub-routine in calculations by certain numerical model as a whole (for details, see PF). To our aims, we can accept the following estimations:

$$RP \cong 0.3 \qquad \text{for} \qquad N_c = 2 \tag{18a}$$

and

$$RP \cong 0.35 \quad \text{for} \qquad N_c = 3 \,. \tag{18b}$$

For the higher values of N_c, estimation of RP requires a use of some software mentioned in the referenced paper. At present it seems that this point is not so important.

For a certain wave energy spectrum, $S(\sigma, \theta)$, the relative error, ϵ_{rel}, is estimated on the basis of comparison of the approximated calculation of the 2-D nonlinear transfer, $T_{ap}(\sigma, \theta)$, and the 'exact' calculation of the same transfer, $T_{ex}(\sigma, \theta)$, for the same wave spectrum at the same 'standard' integration grid (see PF). Herewith, both magnitudes should be expressed in the same dimensional units, whilst the values $T_{ap}(\sigma, \theta)$ should be adjusted to the values $T_{ex}(\sigma, \theta)$ in accordance to the equation

$$\int \left[T_{ex}(\sigma, \theta) - C_{ad}^{(s)} T_{ap}(\sigma, \theta)\right]^2 d\sigma \, d\theta = min \,, \tag{19}$$

where $C_{ad}^{(s)}$ is the adjusting coefficient, and super-index (S) means the dependence of coefficient on a spectrum shape (hereafter this index is omitted). Eventually, in PF-methodic the following estimation of the mean relative error (MRE), ϵ_{rel}, was proposed:

$$\epsilon_{\mathrm{rel}}\left(\Omega_\epsilon\right) = \left[\frac{\int\limits_{\Omega_\epsilon} \left|\frac{T_{ex}(\sigma,\theta) - T_{ap}(\sigma,\theta)}{T_{ex}(\sigma,\theta)}\right| d\sigma \, d\theta}{\int\limits_{\Omega_\epsilon} d\sigma \, d\theta}\right] . \tag{20}$$

Here, Ω_ϵ is the fixed part of the integration frequency-angle space used for the estimation of ϵ_{rel}. In the present work Ω_ϵ

[2] More clarification for the classification of configurations will be done in Sect. 4.

Table 1. A set of parameters for spectra used in calculations

No. of run	f_{p1} , conv.un	θ_{p1} , degrees	γ_1	S_1	$R2$	f_{p2} , conv.un	θ_{p2} , degrees	γ_2	S_2
1	1	0	1	2	0				
2	1	0	1	8	0				
3	1	0	3.3	2	0				
4	1	0	3.3	12	0				
5	1	0	1	8	0.4	2	0	3.3	4
6	1	0	1	8	1.2	2	0	3.3	4
7	1	0	1	8	1.2	2	-60	3.3	4
8	1(swell)	0	3	8	1.2	2	0	3.3	4
9	1(swell)	0	3	8	0.4	2	0	3.3	4

Note: ‘(swell) in the first column means that the first-mode spectrum has the tail of the form: $S_1(f) \propto f^{-10}$.

is corresponding to the 10%–threshold domain defined by the ratio

$$\Omega_\epsilon = \Omega_{10\%} \in |T_{ex}(f,\theta)| \geq 0.1\, R\ , \tag{21}$$

where

$$R = T^+ - T^- \tag{22}$$

and T^+ is the positive extremum of the exact 2-D nonlinear transfer, whilst T^- is the negative one.

Finally, the mean relative error, $< \epsilon_{\rm rel} >$, is estimated as a simple average of the values $\epsilon_{\rm rel}$ obtained for the so-called representative set of spectrum shapes.

According to PF, for the nonlinear transfer calculations the following two-mode spectrum representation has been used[3]

$$S(f,\theta) = S_1(f,\theta,\, f_{p1},\theta_{p1},\gamma_1,s_1) + R2\cdot S_2(f,\theta,\, f_{p2},\theta_{p2},\gamma_{21},s_2)\ , \tag{23}$$

where each of the modes has a typical *JONSWAP* spectrum shape of the kind

$$S(f,\theta,\, f_p,\theta_p,\gamma,s) = \alpha f^{-5}\exp\left(-1.25(f_p/f)^4\right) \cdot\gamma_J^{\exp\left(-(f-f_p)^2/0.01 f_p^2\right)}\Psi(s,\theta,\theta_p)\,. \tag{24}$$

In Eq. (24) the coefficient α is taken to be equal to 1, and the angular spreading function is of the form

$$\Psi(s,\theta,\theta_p) = I_s\cos^s(\theta-\theta_p) \tag{25}$$

with normalization coefficient I_s taken to be equal to 1, for simplicity (as far as the normalized values of the nonlinear transfer is used for comparison). Coefficient $R2$ is responsible for the changing relative intensities of the modes. The extended set of parameters, defining the representative set of the spectra used in our investigations, is presented in Table 1.

[3]In the energy spectrum representation we prefer to use the cyclic frequency, $f = \sigma/2\pi$, instead of the angular one, σ.

Note that all calculations are made on the standard integration grid given by ratios (5) with parameters (7) and $f_0 = \sigma_0/2\pi = 0.7462,\ N = 41,\ M = 36$. The approximated nonlinear transfer for the energy spectrum $S(\sigma,\theta)$ is defined by the typical DIA formulas (Hasselmann et al., 1985):

$$\frac{\partial S(\sigma,\theta)}{\partial t} = I\ (\boldsymbol{k},\boldsymbol{k}_+,\boldsymbol{k}_1,\boldsymbol{k}_2,)\ , \tag{26a}$$

$$\frac{\partial S(\sigma_3,\theta_3)}{\partial t} = I\ (\boldsymbol{k},\boldsymbol{k}_+,\boldsymbol{k}_1,\boldsymbol{k}_2,)\ , \tag{26b}$$

$$\frac{\partial S(\sigma_1,\theta_1)}{\partial t} = -I\ (\boldsymbol{k},\boldsymbol{k}_+,\boldsymbol{k}_1,\boldsymbol{k}_2,)\ , \tag{26c}$$

$$\frac{\partial S(\sigma_2,\theta_2)}{\partial t} = -I\ (\boldsymbol{k},\boldsymbol{k}_+,\boldsymbol{k}_1,\boldsymbol{k}_2,)\ , \tag{26d}$$

where

$$I\ (\boldsymbol{k},\boldsymbol{k}_+,\boldsymbol{k}_1,\boldsymbol{k}_2,) = C\sigma^{11}\Big[S_1S_2(S_3+(\sigma_3/\sigma)^4S_4) - S_3S_4((\sigma_2/\sigma)^4S_1+(\sigma_1/\sigma)^4S_2)\Big] \tag{27}$$

and $S_i = S(\sigma_i,\theta_i)$. The fitting constant C in Eq. (27) is taken to be equal to 1, as far as it finally is merged by the adjusting coefficient C^S_{ad}.

4 A list of the classifications of configurations studied

Due to the discrete nature of configuration parameters, there are, in principle, only a fixed number of configurations that should be tested. For convenience of further consideration, it is worthwhile to classify them in the following manner.

First of all, we distinguish two types of FDIA configuration:

– a simple one (a symbol of the configuration type is S), represented by a set of integer parameters: $m1, m2, m3, n1, n2, n3$, and na (see Sect. 2), and

– a multiple one, which is called a construction (a symbol of the construction is M).

Table 2. Parameters for the set of simple configurations studied

Index of configuration	$m3$ (general)	$m1$	$m2$	$n3$ (general)	na (general)	$n1$	$n2$	$\Delta\theta_{34}$, degree	$\Delta\theta_{a4}$, degree	χ
S1	8	4	5	3	2	2	2	33.2	22.9	4.4
S2*	-"-	4	5	-"-	-"-	3	2	-"-	-"-	-"-
S3	9	5	5	4	3	3	3	37.8	27.0	5.0
S4*	-"-	4	5	-"-	-"-	3	2	-"-	-"-	-"-
S5	10	5	6	4	3	3	3	42.7	31.4	5.6
S6 (or. DIA)	-"-	6	6	-"-	-"-	3	3	-"-	-"-	-"-
S7*	-"-	6	6	-"-	-"-	4	3	-"-	-"-	-"-
S8*	11	6	7	5	4	4	3	47.5	36.1	6.2
S9	-"-	6	6	-"-	-"-	4	4	-"-	-"-	-"-
S10	12	7	7	5	4	4	4	53.1	41.3	6.9
S11	-"-	6	7	-"-	-"-	4	4	-"-	-"-	-"-

Notes. 1. Index of configuration includes the symbol of the configuration type (S or M) and the conventional number of configuration.
2. Configuration S6 is marked as the closest one to the original DIA configuration.
3. Parameters $m3$, $n3$, na are marked as 'general' as far as $m3$ is an independent parameter, and $n3$ and na are directly defined by formulas (13c) and constant for a given $m3$.
4. Super-index '*' means that the configuration is indirect.

Note that in the general case, the M-type constructions include several S-type configurations with different weights, $w1$, $w2$ and so on, which are used instead of factor C in Eq. (27).

In turn, the simple configurations can be shared by subgroups: (a) direct ones, i.e. configurations with equal values of angles θ_1 and θ_2 (equal $n1$ and $n2$); (b) indirect configurations: ones with unequal values of angles θ_1 and θ_2. All M-type constructions can be specified by the number of S-type configurations used in the construction. But it seems that this specification is principally not so.

An experience of the configuration testing shows that the direct configurations conserve total energy, wave action and momentum rather well (conservation errors are less, or of the order of 5–10%), whilst the nonconservativity of the indirect ones is remarkable (especially for the momentum).[4] But, as far as the specially proposed formulas are used for approximation efficiency estimation, conservative features do not play any significant role in our study. Moreover, for some spectrum shapes, the indirect configurations are more efficient than the direct ones.

Analysis of efficiency for different simple configurations permits one to restrict the range of values for parameter $m3$, generating the FDIA configuration as a whole (see below Sect. 5). Due to this, the variety of M-type constructions under consideration is also restricted. The final list of all types of configurations tested is presented in Tables 2 and 3 for simple and multiple FDIA, respectively.

Note that in Table 2, in addition to the integer values $m1, m2, m3, n1, n2, n3$, and na, the exact solutions of Eqs. (10) and (12) and the value

$$x = \ln(\sigma_a/2)/ln(e) \tag{28}$$

are presented for generality and for clarification of the choice for the integer parameters.[5]

In this work we have restricted ourselves by M-type constructions, including only two S-type configurations. The M-type constructions with composition of three or more S-configurations have not been studied in this paper due to the reasons stated below in Sects. 5 and 6.

Table 3. The set of multiple constructions studied

Index of configuration	Composition of simple configurations
M1	$S1+S3$
M2	$S1+S4^*$
M3	$S1+S5$
M4	$S1+0.6^*S5$
M5	$S1+S8$
M6	$S1+0.7^*S8$
M7	$S1+S10$
M8	$S1+0.7^*S10$
M9	$S1+S11$
M10	$S1+0.7^*S11$

[4] For the proper formulas, one may refer to PF.

[5] As one can see, the value x plays the role of the reference value for the choice of $m1$ and $m2$.

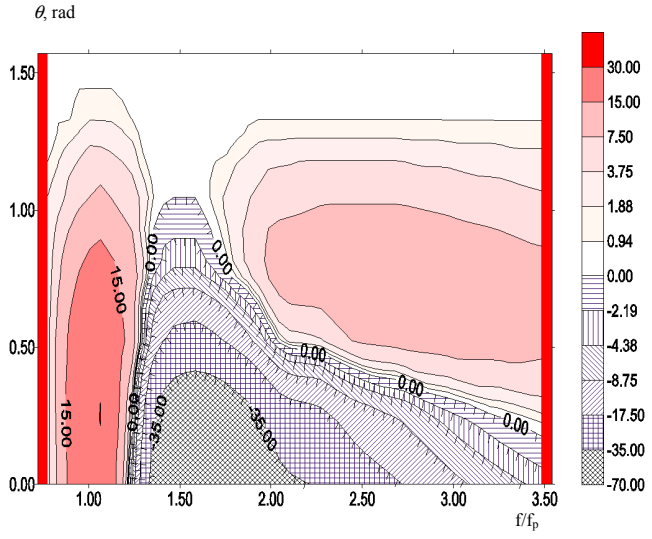

Fig. 2. Two-dimensional topology for the nonlinear transfer of energy (run 1).

5 Results and analysis of the FDIA configurations testing

A typical shape of the 'exact' 2-D nonlinear energy transfer, $T_S(f,\theta)$, is well known (see, for example, Polnikov, 1989). For this, there is no need to dwell here on this point. But to analyze the topology features of approximated transfers, some proper characteristics of $T_S(f,\theta)$ should be introduced. To do this, we use Fig. 2, reproduced from Polnikov (2002).

Based on Fig. 2 and saying in short, we can state that the principal qualitative features of the 2-D Nl-transfer are as follows (Polnikov, 1989):

1. existence of main low-frequency positive lobe (absolute maximum) located along the general spectrum direction (its value earlier was labeled as T^+);

2. existence of main high frequency negative lobe (absolute minimum) located along the general direction (labelled as T^-);

3. existence of two local high frequency lateral positive lobes located symmetrically to the general direction.

Each of the lobes is characterized by a proper frequency and angular width. Values of them, as well as values and locations of these lobes are important quantitative topology features of the transfer. But specification of them is not needed here.

All the features mentioned above take place in the transfers calculated by FDIA. Herewith, locations and values of the lobes are very different from the exact ones, which results in certain relative errors and the efficiency of approximations under study. By just comparing these features we have found natural restrictions for the choice of configurations.

The reference values of the average relative error (ARE) and efficiency was taken as follows:

$$< \epsilon_{\rm rel} >_R = 0.48 \qquad (28a)$$

and

$$Eff_{1R} = 4.3\ , \qquad (28b)$$

which are valid to the FDIA configuration $S5$, corresponding to the original DIA.[6] In the frame of our purpose, only such configurations are of interest which have efficiency parameters that are better than the ones of the reference configuration. Therefore, the testing results are shown only in the proper cases. We now consider separately each type of configurations.

5.1 S-type configurations

Keeping in mind that the original DIA configuration corresponds to the value $m3 \cong 10$, we have started the testing from small values of $m3$, corresponding to the diffusion approximation (DA) considered earlier (Polnikov, 2002; PF). It was found that increasing $m3$ leads to the shifting of both main positive and main negative lobes to the higher frequencies, saving their location at the general direction. Herewith, the local lobes, located near the general direction for small values of $m3$, become more intensively expressed in the lateral directions and also shift to the higher frequencies. This topology change of the 2-D Nl-transfer in FDIA permits one to make a choice of the most effective approximation.

After some attempts it was established that the lowest reasonable value for $m3$ is equal to 8 (configuration $S1$). Some results for $S1$ are presented in Table 4.

The efficiency parameters of the configuration are as follows

$$< \epsilon_{\rm rel} >= 43.6\ , \qquad (29a)$$

$$Eff_1 = 5.26\ . \qquad (29b)$$

Thus, one can see that configuration $S1$ is more effective by 25% than the reference one, $S5$.

The further increase in $m3$ leads to results the best of which correspond to configurations $S3$ and $S4$. They are presented in Tables 5 and 6, respectively. Comparative visual representation of these results is given in Fig. 3.

The efficiency parameters of the last two configurations are as follows. For $S3$ we have:

$$< \epsilon_{\rm rel} >= 44.8\ , \qquad Eff_1 = 4.98\ ; \qquad (30)$$

and for $S4$ to:

$$< \epsilon_{\rm rel} >= 41.4\ , \qquad Eff_1 = 5.82\ ; \qquad (31)$$

Thus, these configurations are also more effective than configuration $S5$, corresponding to the original DIA.

[6] Configuration $S6$ (closest to the original DIA configuration) has worthy efficiency features (see PF).

Table 4. MRE for the FDIA configuration $S1$

No of run	1	2	3	4	5	6	7	8	9
Coefficient C_{ad}	2.99	1.49	2.70	1.68	1.39	1.24	1.70	1.82	1.77
MRE(10%)	36.7	29.8	56.4	35.5	35.9	44.3	56.0	54.0	42.2

Table 5. MRE for the FDIA configuration $S3$

No of run	1	2	3	4	5	6	7	8	9
Coefficient C_{ad}	2.35	1.67	2.94	2.19	1.64	1.47	1.77	2.15	2.79
MRE(10%)	29.8	34.0	57.8	51.4	32.5	41.0	48.5	53.4	55.1

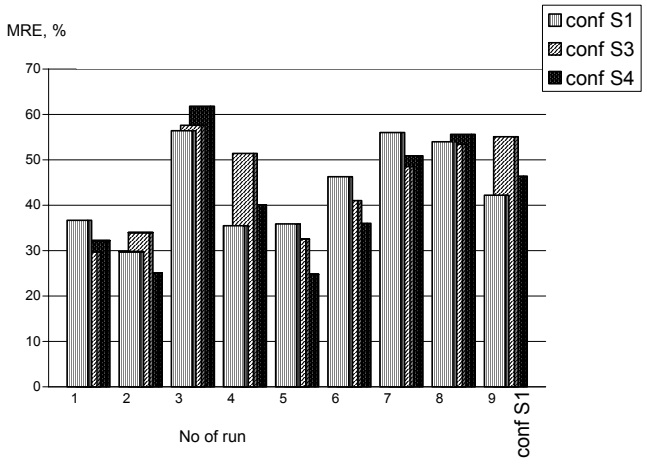

Fig. 3. Comparative diagrams of mean relative errors for configurations $S1$, $S3$, and $S4$. In horizontal axes the number of runs from Table 1 is presented.

Testing all the rest of the configurations presented in Table 2 shows that none of them is more effective than configuration $S5$. For this reason, detailed information for them is not necessary. Nevertheless, they are interesting for the aim of M-type constructions.

Now we touch on configuration properties variety. It is important to mention that a different configuration is the best for a different spectrum shape under consideration. Partially, configuration $S1$ is the best for runs 3, 4 and 9; configuration $S3$ is the best for runs 7 and 8; configuration $S4$ is the best for runs 2, 5 and 6; and configuration $S8^*$ is the best for run 1 (mean relative error $\epsilon_{\rm rel} = 0.12$!). Herewith, configurations $S10$ and $S11$ are more effective than $S8^*$, though they are less effective than $S5$. Just this information initiated making M-type constructions presented in Table 3.

From Table 3 it is evident that all M-constructions are based on configuration $S1$. A preference of using this configuration is provided by the fact that just the spectrum shapes for runs 3, 4, and 9 are the most typical for real wind wave fields. Due to the topology features of S-type configurations, described in the beginning of this sub-section, one should expect that any M-constructions based on $S3$ and $S4$ would be worth in the case of the combinations of two S-type configurations (at least for runs 3 and 4). It is difficult to make the same statement for an M-type construction with three S-configurations. Nevertheless, a hint to such type of conclusion is seen from the results following below.

5.2 M-type constructions of two S-configurations

The efficiency parameters for all the M-constructions considered are presented in Table 7. First of all, it should be noted that practically for all the M-constructions considered, average relative errors (ARE) are less than ones for configurations $S1$, $S3$, and $S4$. Herewith, only the six last constructions have an efficiency better than one for $S4$. Second, the last six constructions have values of ARE which are less than ARE for the M-construction of 3 configurations, presented in our previous paper (PF). Here, we remind the reader that this construction (called as 3C-DIA) has the parameters

$$< \epsilon_{\rm rel} >_{\rm 3C-DIA} = 0.39\,, \quad Eff_2 = 4.4\,. \tag{32}$$

Below, this fact will be used in the discussion of the problem of multiple configuration constructions.

Returning to Table 7 we should note that from a practical point of view only those M-constructions which have the best accuracy are of the most interest. For this reason the detailed results are given only for the four best M-constructions: $M5$, $M6$, $M7$, and $M8$. In a visual form they are presented in Fig. 4.

From the results obtained one may conclude the following:

1. There is no exact regularity in the efficiency parameters of constructions. While changing a form of construction one may improve the accuracy for some spectral shapes, but make worth parameters for other shapes. As a rule, the constructions with rather different values of parameter $m3$ for the S-configurations used are the most effective.

Table 6. MRE for the FDIA configuration $S4$

No of run	1	2	3	4	5	6	7	8	9
Coefficient C_{ad}	1.63	0.99	1.69	1.51	1.00	0.97	1.23	1.29	1.61
MRE(10%)	32.2	25.1	61.8	40.1	24.8	36.0	50.9	55.6	46.4

Table 7. Efficiency parameters for the M-type constructions studied

Index of construc.	M1	M2	M3	M4	M5	M6	M7	M8	M9	M10
ARE	0.416	0.406	0.416	0.413	0.351	0.355	0.355	0.356	0.366	0.364
Eff_1	5.78	6.07	5.78	5.86	8.12	7.93	7.93	7.89	7.46	7.55
Eff_2	4.68	4.91	4.68	4.75	6.57	6.43	6.43	6.39	6.05	6.11

Note. Parameters Eff_1 are related to Eff_2 by the ratio $Eff_2 = 0.81\ Eff_2$ (see Eq. 17). So, the values of Eff_1 are here given for comparison only.

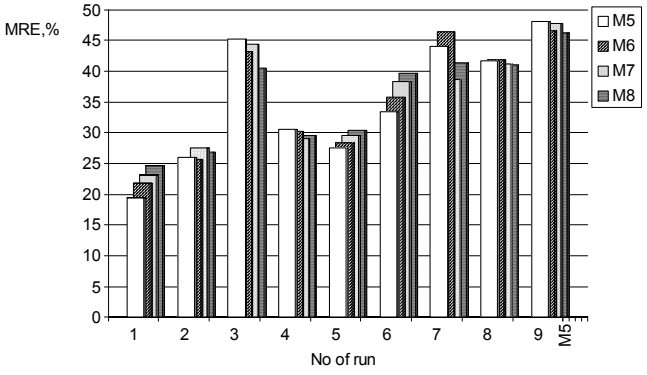

Fig. 4. Comparative diagrams of mean relative errors for constructions $M5$, $M6$, $M7$, and $M8$. For legend, see Fig. 3.

2. The greatest errors take place for the spectra with sharp changes in the shape of the frequency and of the angle (runs 3, 7, 8, and 9). It seems that additional configurations with small values of $m3$ could improve the efficiency of M-construction (though it is not evident at present).

3. The role of weighting coefficients (for the constructions using S-configurations) is not so clear. Partially, construction $M5$ is the best for runs 1, 5, and 6, whilst $M6$ is for run 2; construction $M7$ is the best for runs 4 and 7, and $M8$ is for runs 3, 8, and 9.

4. Due to some small difference between parameters for the last six constructions presented in Table 7, all of them are more or less equivalent in accuracy and efficiency. Thus, to choose the best M-construction among equivalent ones, one needs to specify the preferable spectral shapes under consideration. For practical purposes, the constructions $M7$ and $M8$ can be recommended, as far as they have the best accuracy for runs 3 and 4.

On the basis of these conclusions, one may make some speculations about possibly increasing the efficiency of the approximation by means of increasing the number of S-configurations in the M-construction. This point will be touched on below at the end of Sect. 6, after obtaining some experience in testing the best of configurations found here in the long-term solution of Eq. (1).

6 Some results for long-term spectrum evolution and prospective

As it was mentioned earlier in PF, all the estimations of efficiency presented above are valid only for one time step in the long-term evolution of the wave spectrum, described by Eq. (1). In reality, one should estimate the efficiency of approximation for the long-term evolution as a whole.[7] To do this, one needs to solve Eq. (1) numerically, both in exact and approximated form for the kinetic integral and then to intercompare the features of the spectrum shapes for both cases. Evidently, this is a very complicated task (see remarks in our previous paper). Herewith, this task will partially be fulfilled here by means of intercomparison of some integrated parameters of the spectrum shape, following from the long-term solutions of Eq. (1) for different kinds of approximations.

First of all, we cite the main results of the 'exact' numerical solution of Eq. (1), obtained in Polnikov (1990) and recently confirmed in Lavrenov and Polnikov (2001). They are as follows.

On the time scales of the order of $\tau \geq (10^5 - 10^6)\ f_p^{-1}(0)$ (where $f_p(0)$ is the peak frequency of initial spectrum), the spectrum takes a universal (self-similar) shape, depending

[7] So-called long-term evolution efficiency (PF).

Table 8. Typical spectrum shape parameters for the self-similar solutions of Eq. (1), obtained in different approximations

Type of approximation	Spectrum shape parameter		
	n	δ	A_p
EXACT	7±1	0.25 ±0.03	1.05±0.05
Original DIA	10±1	0.30±0.05	0.65 ±0.05
S-configuration	9 ±0.5	0.28±0.03	0.85±0.1
M-construction	8.5±0.5	0.25 ±0.03	0.9±0.1
ZPA	4.3±0.1	0.75±0.1	1.1±0.1

Note. Results for Zakharov–Pushkarev diffusionApproximation (ZPA) are given from the paper by Polnikov (2002).

slightly on an initial spectral shape. Therefore, one may estimate the long-term efficiency of any approximation by means of comparison of the proper representative spectral parameters for solutions of Eq. (1) at the evolution time $t > \tau$.

In Polnikov (1990) the following features for the self-similar spectral shape were revealed:

(a) the one-dimensional spectrum, $S(f)$, has a tail fall law of the kind $S(f) \propto f^{-n}$ with the value $n = 7 \pm 1$ in the frequency interval $f_p < f < 1.5 f_p$;

(b) the frequency width, δ, defined by the relationship

$$\delta = \int S(f) df / S(f_p) f_p \ , \tag{33}$$

has a small varying value of the order of $\delta = 0.25 \pm 0.03$;

(c) the angle narrowness at the peak frequency, A_p, defined with respect to the general wave propagation direction, θ_p, by the relationship

$$A(f_p) \equiv A_p = S(f_p, \theta_p) / \int S(f_p, \theta) d\theta \ , \tag{34}$$

has a small varying value of the order of $A_p = 1.05 \pm 0.05$.

Thus, the criterion of the approximation quality is an extent of the proper parameters' closeness to the values given above at the evolution time $t > \tau$.

Instead of dwelling on the technical details of the numerical solution for Eq. (1), let us discuss some generalized results for the mentioned parameters, found for the long-term evolution in different approximations. They are presented in Table 8.

The principal long-term features of the approximations are as follows:

1. Original DIA yields too strong a fall of the spectrum tail at higher frequencies, compensated by a rather wide angular spreading in the peak frequency domain;
2. FDIA with the S-configurations gives intermediate result: a more slower tail fall with a more narrower peak frequency domain;
3. FDIA with an M-construction gives the shape of a self-similar spectrum with parameters better corresponding to the exact solution (with respect to FDIA with S-configuration).

In contrary to FDIA, the Zakharov-Pushkarev diffusion Approximation (ZPA), proposed in Zakharov and Pushkarev (1999) and corresponding to the configuration[8]

$$\boldsymbol{k}_1 \cong \boldsymbol{k}_2 \cong \boldsymbol{k}_3 \cong \boldsymbol{k}_4 \ , \tag{35}$$

gives the spectrum shape with too slow a tail fall, which is compensated by the extremely narrow angular spreading at the peak frequency domain (for details, see Polnikov, 2002).

Finally, one may conclude that FDIA with M-constructions and S-configurations really has a long-term efficiency that is better than the efficiency of the original DIA. Despite the rather small difference for spectrum shape parameters found for these approximations, the results obtained confirm our previous conclusion about the better efficiency of the approximations constructed. Moreover, it seems that the efficiency of FDIA could be enhanced, if one includes into the M-construction some additional S-configurations with small values of configuration parameter $m3$ (which are corresponding to configuration (35)). This work could be made in the future.

For the sake of the paper let us say several words about possible future work. The topology basis for making better M-constructions is related to the better reproduction of locations and values for main positive and negatives lobes of the 2-D NL-transfer (see, Fig. 2). From a first glance, it seems that a simple addition of any S-configuration should lead to improving the features of M-constructions. But the results of testing show that this is not true (compare efficiency parameters for $M7(S1 + S10)$ in Table 7 to the one for 3C-DIA in Eq. (32); the latter corresponds to M-construction $(S1 + S5 + S10)$. It is evident that the weighting coefficients here play the key role. The choice of the coefficients is very cumbersome work.

Moreover, the optimal number of S-configurations in the M-construction is not known. It should not be so great as to restrict the time of the one-step calculation and the value of RP (see Eq. 17), yet not so small as to provide a proper decreasing ARE. All these details make for a rather unclear prospective of seeking an effective M-construction with three or more S-configurations. For this reason this point was not elaborated in the present paper.

7 Conclusions and recommendations

In this paper the main ideas of the Fast Discrete Interaction Approximation (FDIA) to the kinetic integral, proposed earlier in PF, were elaborated and clarified. Classification of

[8] For details, see PF.

the discrete configurations was given, and many of examples of simple (S-type) and multiple (M-type) FDIA have been tested in the frame of the PF method, with the aim of choosing the optimal approximation.

It was found that three S-configurations are more effective than the original DIA configuration. The best of them are configurations $S1$ and $S4$, having an efficiency value 1.5 times greater than the one for the original DIA. Both of them may be recommended for implementation into wind-wave forecasting practice.

Additionally, six M-constructions of two S-configurations were found to have an efficiency better than the best of the S-configuration, $S4$. Four of them, $M5$, $M6$, $M7$, and $M8$, may be recommended for implementation.

The better long-term efficiency derived of the S-configurations and M-constructions was confirmed on the basis of intercomparison between the relevant integrated parameters of wave spectrum shape, following from the long-term solutions of Eq. (1). The prospective of seeking an effective M-construction with three or more S-configurations was discussed.

Acknowledgements. The author is grateful to the administration of CPTEC and CNPq of the Brazil for the funding this work. In part this work was supported by the Russian Fund for Basic Research, project # 05-01-64580.

References

Hashimoto, N. and Kawagushi, K.: Extension and modification of the Discrete Interaction Approximation (DIA) for computing nonlinear energy transfer of gravity wave spectra, Proc. 4th Int. Symp. on Ocean Waves, Measurement and Analysis, WAVES-2001, 530–539, 2001.

Hasselmann, K.: On the non-linear energy transfer in a gravity wave spectrum, Pt.1. General theory, J. Fluid Mech., 12, 481–500, 1962.

Hasselmann, S., Hasselmann, K., Allender, K. J., and Barnett, T. P.: Computations and parameterizations of the nonlinear energy transfer in a gravity-wave spectrum, Part II, J. Phys. Oceanogr., 15, 1378–1391, 1985.

Komen, G. J., Cavaleri, L., Donelan, M., et al.: Dynamics and Modeling of Ocean Waves, N.Y., Cambridge University Press, 532, 1994.

Lavrenov, I. V. and Polnikov, V. G.: A study of properties for non-stationary solutions of the Hasselmann's kinetic equation, Izvestiya, Atmos. Oceanic. Phys., 37, 661–670, (English translation), 2001.

Polnikov, V. G.: Calculation of the nonlinear energy transfer through the surface gravity waves spectrum, Izv. Acad. Sci. SSSR, Atmos. Oceanic. Phys., 25, 896–904, (English translation), 1989.

Polnikov, V. G.: Numerical solution of the kinetic equation for surface gravity waves, Ibid., 26, 118–123, (English translation), 1990.

Polnikov, V. G.: A Basing of the Diffusion Approximation Derivation for the Four-Wave Kinetic Integral and Properties of the Approximation, Nonlin. Proc. Geophys., 9, 355–366, 2002.

Polnikov, V. G. and Farina, L.: On the problem of optimal approximation for the four-wave kinetic integral, Nonlin. Proc. Geophys., 9, 497–512, 2002.

Zakharov, V. E. and Pushkarev, A.: Diffusion model of interacting gravity waves on the surface of deep fluid, Nonlin. Proc. Geophys., 6, 1–10, 1999.

Van Vledder, G. Ph.: Extension of the Discrete Interaction Approximation for computing nonlinear quadruplet wave-wave interactions in operational wave prediction model, Proc. 4th Int. Conf. on Ocean Waves. WAVES-2001, San Fransisco, Sept., 540–549, 2001.

Young, I. R. and Van Vledder, G. Ph.: The Central Role of Nonlinear Interactions in Wind-wave Evolution, Phil. Trans. Roy. Soc. Lond., A 342, 505–524, 1993.